Contents lists available at ScienceDirect

Artificial Intelligence in the Life Sciences

journal homepage: www.elsevier.com/locate/ailsci

Research Article

Machine learning for longitudinal mortality risk prediction in patients with malignant neoplasm in São Paulo, Brazil

GFS Silva[a,*], LS Duarte[b], MM Shirassu[b], SV Peres[c], MA de Moraes[b], A Chiavegatto Filho[a]

[a] *School of Public Health, University of São Paulo, São Paulo, Brazil*
[b] *São Paulo State Health Department, Division of Non-communicable diseases, São Paulo, Brazil*
[c] *São Paulo State Health Department, Oncocenter Foundation of São Paulo, São Paulo, Brazil*

ARTICLE INFO

Keywords:
Machine learning
Artificial intelligence
Predictive model
Cancer

ABSTRACT

Artificial intelligence is becoming an important diagnostic and prognostic tool in recent years, as machine learning algorithms have been shown to improve clinical decision-making. These algorithms will have some of their most important applications in developing regions with restricted data collection, but their performance under this condition is still widely unknown. We analyzed longitudinal data from São Paulo, Brazil, to develop machine learning algorithms to predict the risk of death in patients with cancer. We tested different algorithms using nine separate model structures. Considering the area under the ROC curve (AUC-ROC), we obtained values of 0.946 for the general model, 0.945 for the model with the five main cancers, 0.899 for bronchial and lung cancer, 0.947 for breast cancer, 0.866 for stomach cancer, 0.872 for colon cancer, 0.923 for rectum cancer, 0.955 for prostate cancer, and 0.917 for uterine cervix cancer. Our results indicate the potential of building models for predicting mortality risk in cancer patients in developing regions using only routinely-collected data.

1. Introduction

Neoplasms are defined by abnormal tissue growth and can be classified as benign or malignant. Benign (noncancerous) neoplasms are characterized by slow and organized spread, the presence of well-defined borders, and the absence of an invasive character at both the tissue and organ levels. Malignant (cancerous) neoplasms, on the other hand, are characterized by often rapid and disorganized growth, with poorly defined borders and possible invasion of adjacent tissues and organs, implying the possibility of metastatic cancer [1,2].

According to the World Health Organization, about 9.6 million people died of cancer worldwide in 2018, of which around 70% were in middle- and low-income countries [3]. In Brazil, according to the National Cancer Institute (INCA) [4], about 625,000 new cases were expected in 2020, based on estimates from before the SARS-coV-2 pandemic, and were mainly distributed among cancers of the prostate, female breast, colon and rectum, trachea, bronchus and lung, and stomach. As for the total number of deaths, according to the Brazilian Mortality Information System data (SIM), 224,829 deaths were caused by malignant neoplasms in 2020, and the most frequent were trachea, bronchus, and lung (28,516 deaths), breast (18,032 deaths), prostate (15,841 deaths), stomach (13,850 deaths), and colon (12,422 deaths) [5].

Artificial Intelligence (AI) has become an important tool in the field of medicine. Machine learning algorithms are capable to identify patterns and trends from data that may not be readily apparent to the human eye. This allows medical professionals to make more accurate predictions about patient diagnosis and prognosis and make informed decisions about their treatment. Machine learning in healthcare has the potential to greatly improve patient outcomes and make the healthcare system more efficient.

Given the growing scenario of cancer cases in Brazil and around the world [4,6], it is increasingly important to improve prognostic decisions for cancer patients [7]. The aim of this work is to develop machine learning algorithms to predict the risk of death in cancer patients in order to provide inputs for their clinical management.

2. Material and methods

2.1. Dataset description

We analyzed data collected from the Hospital Cancer Registry (RHC) of the Oncocenter Foundation of São Paulo (FOSP/SP) [8], a public registry that monitors patients treated in the state of São Paulo since the year 2000. RHC has information on the cancer diagnosis, treatment, metastases, recurrences, age and sex of the patients, and data on the

[*] Corresponding author.
E-mail address: gabriel8.silva@usp.br (G. Silva).

https://doi.org/10.1016/j.ailsci.2023.100061
Received 21 December 2022; Received in revised form 31 January 2023; Accepted 1 February 2023
Available online 3 February 2023

health facilities/organizations where the consultations were performed. The dataset includes a total 99 variables and 1085,380 patients from 2000 through September 2022.

All variables collected after the cancer diagnosis for each patient were removed. The algorithms were trained with twelve variables: sex, age, days between first physician visit and diagnosis, clinical stage of cancer, category of medical service, previous diagnosis, type of diagnosis, topography group, health region of residence [9], morphology, health institution habilitation, and health region of diagnosis. There are three levels to the variable category medical service: 1) private care, 2) public care, 3) private care. The variable previous diagnosis presents binary information, 1 for patients who started longitudinal follow-up with a previous cancer diagnosis and 0 for patients without previous diagnosis. The variable type of diagnosis presents four categories: 1) clinical examination, 2) non-microscopic auxiliary resources, 3) microscopic confirmation and 4) no information. The variables cancer topography and cancer morphology are categorized with ICD-10 and ICD-O, respectively. The variables related to health region have seventeen distinct values, referring to the seventeen health regions in the state of São Paulo, Brazil. The variable health institution habilitation has fifteen categories: 1) High Complexity Oncology Care Unit (UNACON), 2) UNACON with Radiotherapy Service, 3) UNACON with Hematology Service, 5) Exclusive UNACON for Pediatric Oncology, 6) High Complexity Oncology Care Center (CACON), 7) CACON with Pediatric Oncology Service, 8) General Hospital with Oncological Surgery, 9) UNACON with Radiotherapy and Hematology Services, 10) UNACON with Radiotherapy, Hematology and Pediatric Oncology Services, 12) UNACON with Hematology and Pediatric Oncology Services, 13) Volunteer, 14) Inactive, 15) Exclusive UNACON for Pediatric Oncology with Radiotherapy Service. The full description of the dataset and its variables can be found in Supplementary Appendix B (Table B1).

Only patients with diagnoses from 2014 to 2017 were included, in order to avoid longer clinical effects after the diagnosis. Although the dataset included a small portion of population from other Brazilian states, we limited the algorithm development to residents of the state of São Paulo (93% of total patients). We included only patients with malignant neoplasms and excluded cases of non-melanoma of the skin as they had a low mortality rate. We analyzed adult patients regardless of sex. The final sample was composed of a total of 29,194 patients.

2.2. Outcome definition

The original dataset contains four categories regarding the last available information about the patient: 1) alive without cancer, 2) alive with cancer, 3) death from cancer, and 4) death without further information. Our outcome of interest was patients with a confirmed cancer death between 12 and 24 months after the date of diagnosis. For the negative outcome, we included patients 1) alive without cancer or 2) alive with cancer between 12 and 36 months after the date of diagnosis. Patients were removed if categorized as 4) death without other information.

2.3. Model design

Considering the distinct cancer types, we tested different models to assess whether changing the strategy increased model performance. We first developed a general model for all cancer types. We then developed a model for the top five causes of cancer mortality (bronchus and lung, breast, stomach, colon, and rectum). We also trained specific models for the five most frequent causes and added two other models based on its growing importance for health vigilance: prostate cancer and cervix uteri cancer (in both cases the sex variable was not used as a predictor). We evaluated the models independently, without sharing any information during algorithm training. A summary of the model design is provided in Supplementary Appendix A (Figure A1).

2.4. Machine learning techniques

For quantitative variables, we performed normalization using the z-score (separately in training and test). For all qualitative variables, we separated each category using one-hot encoding. The variable type of diagnosis presented categorized missing (value 9) for twenty-four patients. We considered this a new category for the one hot encoding procedure. We also removed 75 patients due to the lack of any information in two variables: cancer stage (two patients) and difference in days between first medical appointment dates and diagnosis (73 patients).

We tested the predictive performance of six different machine learning algorithms: catboost [10], xgboost [11], lightgbm [12], gradient boosting classifier, random forest, logistic regression. For catboost, xgboost and lightgbm, we used their own Python packages. For the other algorithms, we used the scikit-learn library [13].

We used 10-fold cross-validation to select the hyperparameters in the training set with Hyperopt [14], which applies a Bayesian strategy for optimization, and RandomSearch. In the case of high class imbalance (minority class representing under 25% of total outcomes), we applied the Synthetic Minority Oversampling Technique (SMOTE). Also in the training set, we applied the BORUTA [15] method for variable selection.

We then selected the best performing models from the training set (70% of the data) to evaluate their performance in the test set (30%). The complete structure of the datasets is presented in Fig. 1.

The predictive performance of the models was evaluated on the test set using metrics such as area under the ROC curve (AUC-ROC), area under the precision-recall curve (AUC-PR), precision, recall, positive predicted value, negative predicted value, and F1-score. We also evaluated the performance of the algorithms in the 20% highest risk patients (20% k-tops), with metrics such as true positive, false positive, precision and recall. Finally, the interpretation and evaluation of the contribution of each variable to the outcome was obtained by calculating the Shapley values [16,17,18] for the test set. We followed the guidelines of the transparent reporting of a multivariable prediction model for individual prognosis or diagnosis (TRIPOD) [19].

3. Results and discussion

3.1. Descriptive data analysis

After data preprocessing, a total 29,194 patients were included in the study, most of whom were female (51.0%). A total of 27.7% of patients were between 60 and 69 years old and 23.5% seventy or more. Regarding the clinical classification of the cancer, there was a relative balance between stages I (20.9%), II (20.3%), III (20.1%), IV (26.0%). The other categories accounted for about 12.6% of the total number of patients.

Regarding the category of health services, 72.7% of patients were diagnosed in public institutions, 26.6% in private services and 0.7% in individual private services. Of the total patients, 43.6% died between 12 and 24 months after the date of the malignant cancer diagnosis and 56.4% remained alive. The characteristics of the patients were similar in the training and testing data, as well as in the general dataset (Table 1). Additional summaries of cancer morphology and topography are provided in Tables B2 and B3 in Supplementary Appendix B.

3.2. Model data structure

We developed a total of 42 machine learning algorithms considering nine root structures: 1) general model, 2) top 5 cause of death model, 3) bronchus and lung cancer model, 4) breast cancer model, 5) stomach cancer model, 6) colon cancer model, 7) rectum cancer model, 8) prostate cancer model, and 9) cervix uteri cancer model. Table 2 provides a descriptive summary of each model considering the total number of patients, total number of deaths and nondeaths, total mortality, and

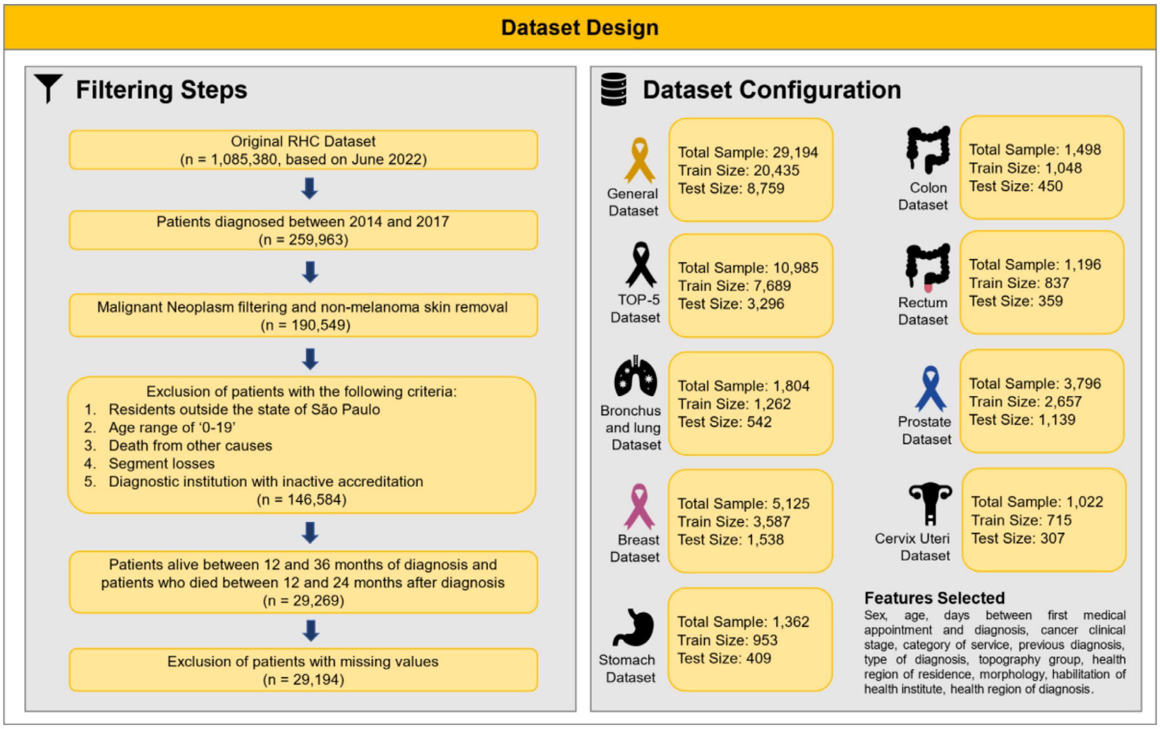
Dataset Design

Filtering Steps

Original RHC Dataset
(n = 1,085,380, based on June 2022)

Patients diagnosed between 2014 and 2017
(n = 259,963)

Malignant Neoplasm filtering and non-melanoma skin removal
(n = 190,549)

Exclusion of patients with the following criteria:
1. Residents outside the state of São Paulo
2. Age range of '0-19'
3. Death from other causes
4. Segment losses
5. Diagnostic institution with inactive accreditation
(n = 146,584)

Patients alive between 12 and 36 months of diagnosis and patients who died between 12 and 24 months after diagnosis
(n = 29,269)

Exclusion of patients with missing values
(n = 29,194)

Dataset Configuration

General Dataset: Total Sample: 29,194; Train Size: 20,435; Test Size: 8,759

TOP-5 Dataset: Total Sample: 10,985; Train Size: 7,689; Test Size: 3,296

Bronchus and lung Dataset: Total Sample: 1,804; Train Size: 1,262; Test Size: 542

Breast Dataset: Total Sample: 5,125; Train Size: 3,587; Test Size: 1,538

Stomach Dataset: Total Sample: 1,362; Train Size: 953; Test Size: 409

Colon Dataset: Total Sample: 1,498; Train Size: 1,048; Test Size: 450

Rectum Dataset: Total Sample: 1,196; Train Size: 837; Test Size: 359

Prostate Dataset: Total Sample: 3,796; Train Size: 2,657; Test Size: 1,139

Cervix Uteri Dataset: Total Sample: 1,022; Train Size: 715; Test Size: 307

Features Selected

Sex, age, days between first medical appointment and diagnosis, cancer clinical stage, category of service, previous diagnosis, type of diagnosis, topography group, health region of residence, morphology, habilitation of health institute, health region of diagnosis.

Fig. 1. Dataset filtering and configurations for predictive models' development.

Table 1
Descriptive summary of full, train and test datasets.

Variable	Full Dataset	Death	Non-death	Train	Test
Sex					
Male	14,313 (49.0%)	7027 (55.2%)	7286 (44.2%)	9972 (48.8%)	4341 (49.6%)
Female	14,881 (51.0%)	5697 (44.8%)	9184 (55.8%)	10,463 (51.2%)	4418 (50.4%)
Age					
20–29	929 (3.2%)	263 (2.1%)	666 (4.0%)	652 (3.2%)	277 (3.2%)
30–39	2176 (7.5%)	636 (5.0%)	1540 (9.4%)	1534 (7.5%)	642 (7.3%)
40–49	3862 (13.2%)	1453 (11.4%)	2409 (14.6%)	2714 (13.3%)	1148 (13.1%)
50–59	7270 (24.9%)	3234 (25.4%)	4036 (24.5%)	5077 (24.8%)	2193 (25.0%)
60–69	8093 (27.7%)	3690 (29.0%)	4403 (26.7%)	5658 (27.7%)	2435 (27.8%)
70+	6864 (23.5%)	3448 (27.1%)	3416 (20.7%)	4800 (23.5%)	2064 (23.6%)
Clinical Stage					
I	6107 (20.9%)	570 (4.5%)	5537 (33.6%)	4292 (21.0%)	1815 (20.7%)
II	5917 (20.3%)	1371 (10.8%)	4546 (27.6%)	4119 (20.2%)	1798 (20.5%)
III	5876 (20.1%)	2843 (22.3%)	3033 (18.4%)	4088 (20.0%)	1788 (20.4%)
IV	7602 (26.0%)	6090 (47.9%)	1544 (9.4%)	5361 (26.2%)	2241 (25.6%)
X	712 (2.4%)	414 (3.3%)	1512 (9.2%)	482 (2.4%)	230 (2.6%)
Y	2980 (10.2%)	1436 (11.3%)	298 (1.8%)	2093 (10.2%)	887 (10.1%)
Service Category					
Public	21,224 (72.7%)	11,865 (93.2%)	9359 (56.8%)	14,840 (72.6%)	6384 (72.9%)
Private	7755 (26.6%)	803 (6.3%)	6952 (42.2%)	5448 (26.7%)	2307 (26.3%)
Particular	215 (0.7%)	56 (0.4%)	159 (1.0%)	147 (0.7%)	68 (0.8%)
utcome					
Death	12,724 (43.6%)	–	–	8906 (43.6%)	3818 (43.6%)
Non-death	16,470 (56.4%)	–	–	11,529 (56.4%)	4941 (56.4%)

the number of patients in the training and test groups. There were notable imbalances according to the different models, with 29,194 patients in the general model and 1022 in the cervix uteri cancer model, which may have affected the predictive performance of the algorithms.

3.3. Algorithms performance

The catboost algorithm presented the best performance on all models except stomach, where Gradient Boosting performed better in terms of AUC-ROC. Fig. 2 presents the performance of the best prediction algorithms for each of the models considering the AUC-ROC test set criterion (a) and AUC-PR (b). We found good discrimination performance for the nine models. All models presented AUC-ROC values of at least 0.871 and six of them reached values above 0.900. The general model presented the best overall performance, with AUC-ROC of 0.946 and AUC-PR of 0.932. The model for the five main causes of death (top-5) presented an AUC-ROC of 0.945 and an AUC-PR of 0.937.

In the general model, we tested combinations of hyperparameter optimization (Hyperopt and RandomSearch) and variable selection (BORUTA). However, the best predictive performance was achieved for the raw model, with AUC-ROC of 0.946, recall 0.855, specificity 0.889, precision 0.857, F1-score 0.856, and AUC-PR 0.932 (Table 3). Although changes in algorithm settings improved at least one scoring metric (i.e., the general model with RandomSearch had a recall of 0.858), the raw

Table 2
Description of the eight models developed for prediction of cancer mortality.

ID	Model	Variables	Total cases	Non-death	Death	Mortality rate	Train Size (70%)	Test Size (30%)
1	General	sex, age, medsvtodiag, cancerstage, servicecat, prevdiag, diagbase, topogroup, rras, morpho, habilit, rrasofserv	29,194	16,470	12,724	43.6%	20,435	8.759
2	Top-5 cause of death	sex, age, medsvtodiag, cancerstage, servicecat, prevdiag, diagbase, topogroup, rras, morpho, habilit, rrasofserv	10,985	5937	5048	46.0%	7689	3.296
3	Bronchus and lung	sex, age, medsvtodiag, cancerstage, servicecat, prevdiag, diagbase, rras, morpho, habilit, rrasofserv	1804	468	1336	74.1%	1262	542
4	Breast	sex, age, medsvtodiag, cancerstage, servicecat, prevdiag, diagbase, rras, morpho, habilit, rrasofserv	5125	3845	1280	25.0%	3587	1.538
5	Stomach	sex, age, medsvtodiag, cancerstage, servicecat, prevdiag, diagbase, rras, morpho, habilit, rrasofserv	1362	401	961	70.6%	953	409
6	Colon	sex, age, medsvtodiag, cancerstage, servicecat, prevdiag, diagbase, rras, morpho, habilit, rrasofserv	1498	740	758	50.6%	1048	450
7	Rectum	sex, age, medsvtodiag, cancerstage, servicecat, prevdiag, diagbase, rras, morpho, habilit, rrasofserv	1196	483	713	59.6%	837	359
8	Prostate	age, medsvtodiag, cancerstage, servicecat, prevdiag, diagbase, rras, morpho, habilit, rrasofserv	3796	3232	664	17.5%	2657	1.139
9	Cervix uteri	age, medsvtodiag, cancerstage, servicecat, prevdiag, diagbase, rras, morpho, habilit, rrasofserv	1022	416	609	59.6%	715	307

medsvtodiag: difference in days between first medical appointment dates and diagnosis, **cancerstage**: cancer clinical stage, **servicecat**: category of service, **prevdiag**: previous diagnosis, **diagbase**: type of diagnosis, **topogroup**: cancer topography, **rras**: regional net of healthcare (residence), **morpho**: cancer morphology, **habilit**: qualification of the health establishment, **rrasofserv**: regional net of healthcare (service).

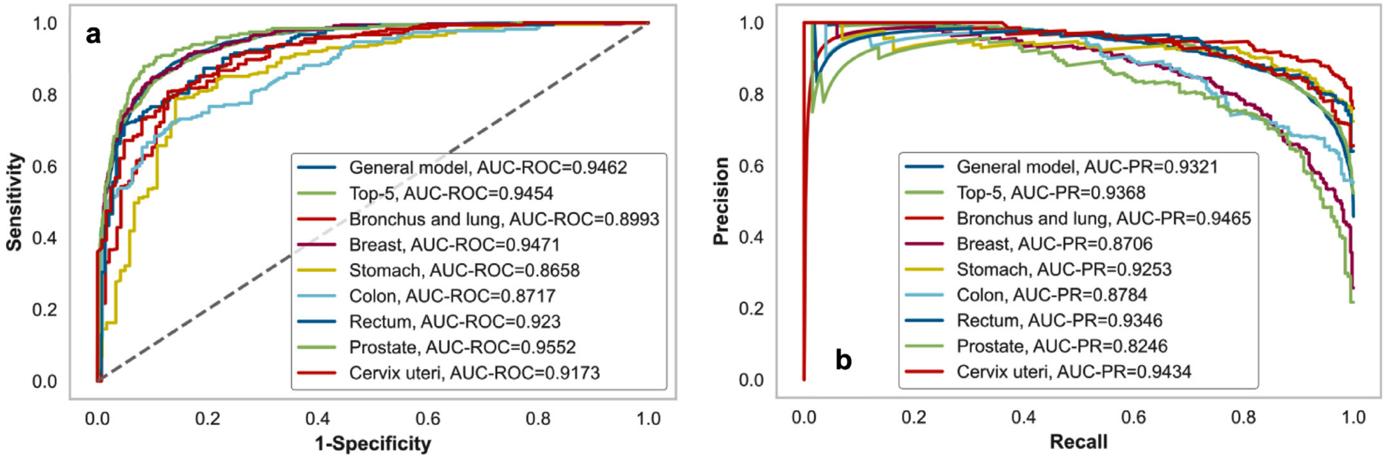

Fig. 2. Predictive performance of best algorithm for each model regarding AUC-ROC (a) and AUC-PR (b).

Table 3
Predictive performance of best algorithm for each model.

ID	Model	Best Algorithm	Hypermeter Tunning	Feature Selection	Resample	Accuracy	AUC-ROC	Recall	Specificity	Prec.	F1	AUC-PR
1	General	CatBoost Classifier	None	None	None	0.8743	0.9462	0.8549	0.8893	0.8565	0.8557	0.9321
2	Top-5 cause of death	CatBoost Classifier	None	None	None	0.8686	0.9454	0.8581	0.8776	0.8564	0.8572	0.9368
3	Bronchus and lung	CatBoost Classifier	None	None	SMOTE	0.8561	0.8993	0.9152	0.6879	0.8929	0.9039	0.9465
4	Breast	CatBoost Classifier	None	None	None	0.8973	0.9471	0.7214	0.9558	0.8445	0.7781	0.8706
5	Stomach	Gradient Boosting	RandomSearch	None	None	0.8093	0.8658	0.9343	0.5083	0.8207	0.8738	0.9253
6	Colon	CatBoost Classifier	None	None	None	0.7578	0.8717	0.7763	0.7387	0.7532	0.7646	0.8784
7	Rectum	CatBoost Classifier	Hyperopt	None	None	0.8412	0.9230	0.9159	0.7310	0.8340	0.8731	0.9346
8	Prostate	CatBoost Classifier	None	None	None	0.9210	0.9552	0.7487	0.9574	0.7884	0.7680	0.8246
9	Cervix uteri	CatBoost Classifier	Hyperopt	None	None	0.8306	0.9173	0.9235	0.6935	0.8164	0.8667	0.9434

Table 4
Predictive performance of best algorithm for each model based on 20% individuals with the highest risk of death.

ID	Model	Total Patients	Real Positive	Positive Prediction	True Positive	False Positive	Precision	Recall
1	General	1749	1703	1749	1703	46	0.9737	1.0000
2	Top-5 cause of death	659	645	659	645	14	0.9788	1.0000
3	Bronchus and lung	109	107	109	107	2	0.9817	1.0000
4	Breast	308	263	308	263	45	0.8539	1.0000
5	Stomach	82	78	82	78	4	0.9512	1.0000
6	Colon	90	88	90	88	2	0.9778	1.0000
7	Rectum	72	70	72	70	2	0.9722	1.0000
8	Prostate	228	166	189	149	40	0.7884	0.8976
9	Cervix uteri	62	60	62	60	2	0.9677	1.0000

model was the one that presented the best AUC-ROC. When BORUTA was used, there was a significant reduction in the number of predictors (497 to 93) without a large loss in predictive performance (AUC-ROC of 0.946 for the raw model versus 0.945 for the model with BORUTA and without hyperparameter optimization). A similar pattern to the general model was observed for the top 5 causes of death model. Complete results for all training strategies can be found in Supplementary Appendix B (Table B4). The hyperparameters of each model are also available in Supplementary Appendix B (Tables B5, B6, B7, B8, B9, B10, B11, B12, B13).

We also evaluated the performance of the algorithms in the top 20% (20% k-tops) of patients with the highest mortality risk (Table 4). The general model had 1749 patients in the group, of whom 1703 died, giving the algorithm a precision of 97,37% and a recall of 100% in this high-risk group. For the top 5 causes of death model, 659 individuals were in the 20% highest risk patients, of which 645 died, resulting in a precision of 97.88% and a recall of 100%.

3.4. Model interpretation

In order to interpret the decision-making process of the algorithms, we calculated the Shapley values. In the general model (Fig. 3), the cancer stage during the first diagnosis was the most important predictor. Stage I patients were more likely to be classified negatively (non-death), whereas stage IV patients were more significant for the positive outcome (death). The variable on the category of service provided was also important for the outcome. Category 2 (public service) increased mortality prediction, whereas category 1 (private service) showed a greater propensity for patient survival. The other main predictive variables refer to the topography of cancer, regional net of healthcare service (rrasofserv) and regional net of healthcare service (rras). The plots of Shapley values for the other models can be found in Supplementary Appendix A (Figures A2, A4, A6, A8, A10, A12, A14, A16).

We also randomly selected three patients (high risk, medium risk, and low risk) to highlight the individual interpretation of results (Fig. 4). The first (a) was a true positive (risk of 0.972) with the expected Shapley value was 2.92. The variables that contributed for the prediction of positive outcome were public care service (servicecat_2 = 1), cancer stage different from I (cancerstage_*I*= 0), cancer topography ICD C-34 (malignant neoplasm of bronchus and lung), regional net of service 01 (rrasofserv_RRAS01 = 1) and the qualification of the healthcare institution (code 12, UNACON with Hematology and Pediatric Oncology Services). A second patient (b) classified as a false negative was selected. The total risk score was 0.4782, which led the algorithm to classify the patient incorrectly as alive during the period. We observed that there was balance in the aggregate of the contribution of the predictors, highlighting the importance of cancer stage IV to increase Shapley value and the non-public health service to decrease it. For patient c, a true negative classified as low risk, the most important characteristic to a low expected Shapley value were cancer stage I and non-public health service. Visualizations of the individual Shapley values for the other models are available in Supplement A (figures A3, A5, A7, A9, A11, A13, A15, A17).

3.5. General vs specific models

To understand the best strategy regarding the types of models (general or specific for each cancer), we performed a comparison between the performance of the general algorithm for all cancers versus the specific algorithms for bronchus and lung, breast, stomach, colon, rectum, prostate, bronchus and lung, colon, and uterine cervix (Table 5). Based on the AUC-ROC, the general model performed better in bronchus and long, stomach and colon. For breast, rectum, prostate, and cervix uteri the model performed better for the specific case. For bronchus and lung cancer, the area under the curve increased from 0.899 (model specific) to 0.927 (general model) and the precision from 0.893 to 0.907. For stomach cancer, there was an increase in AUC-ROC (0.866 to 0.926), precision (0.821 to 0.924). This scenario was repeated for colon cancer (AUC-ROC 0.753 to 0.848).

3.6. Discussion

We found that all models achieved an AUC-ROC higher than 0.86 to predict cancer mortality using only routinely-collected data. Our results also indicated that a general algorithm, that included all cancer mortality, performed in most cases better than cancer-specific algorithms.

Information about mortality risk after cancer diagnosis can be an important input to support clinical decisions. These algorithms can be integrated into mobile devices, electronic medical records, or online resources, to help doctors in making more informed decisions about treatment options and to allocate healthcare resources more effectively.

We obtained a high predictive performance without the use of omics or image data, which is a promising result in the field of oncology especially in low-income regions. We were able to develop an approach to compare the use of a general model with a model for the main causes of death, and with models specific to each type of cancer. Most of the studies developed in the literature are specific for a given type of cancer, due to the selected data sets, using either from image data or through structured data [20,21]. The use of data from a cancer registry allowed for achieving consistent results in all proposed models, while at the same time providing a real-world dataset, with recent cases and different types of cancer.

The study has a few limitations. First, the algorithms were developed with data from São Paulo, Brazil, so there should be caution in transferring its conclusions to other contexts. Second, considering the filtered sample, we had 1391 follow-up losses that could have disproportionally altered the results. Third, we excluded patients younger than 20 years due to the presence of different biological mechanisms that lead to cancer deaths for this group, so the results refer only to adult patients.

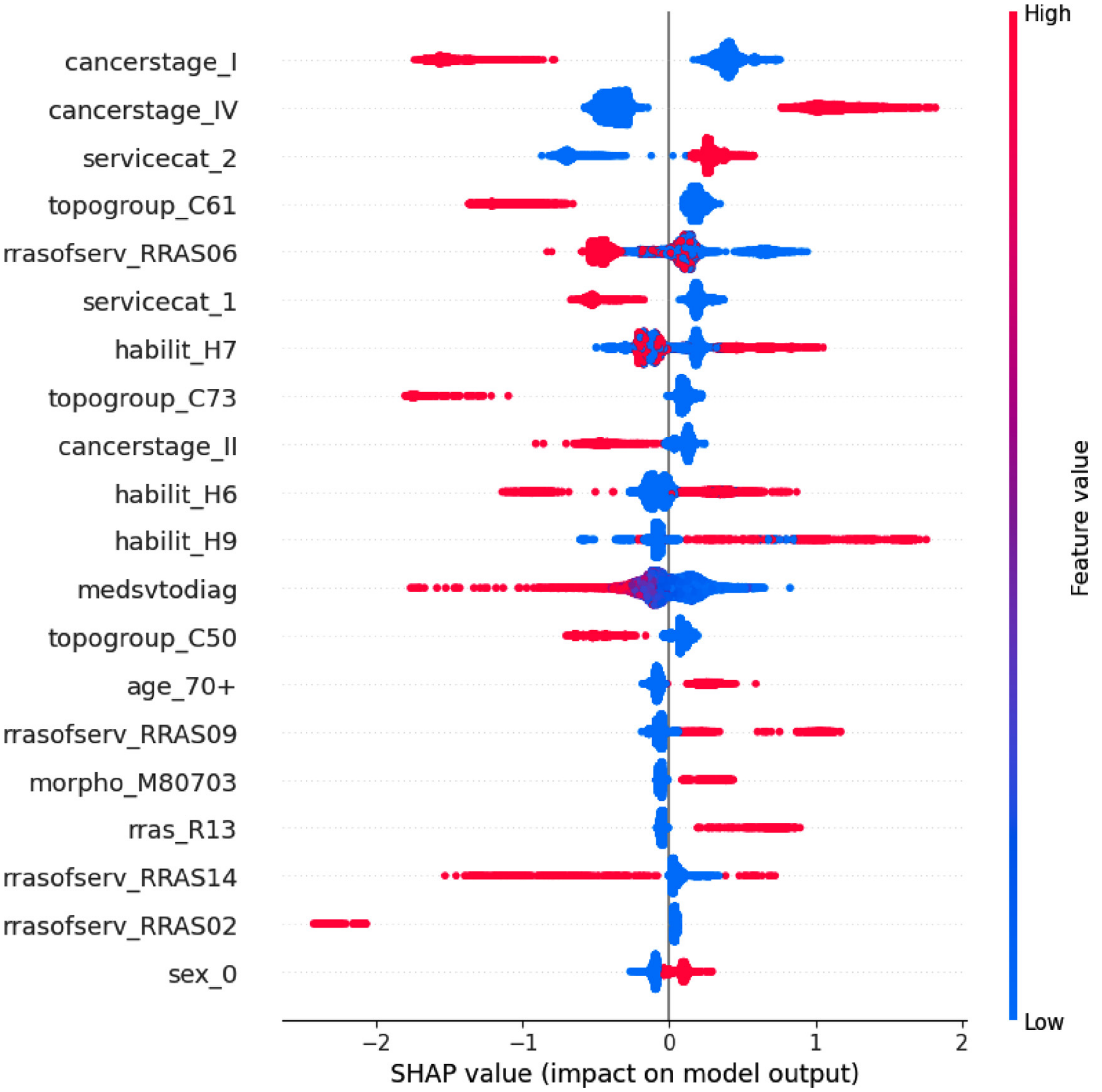

Fig. 3. Top twenty predictors of risk of death from cancer 12 to 24 months after diagnosis. General Model, with Catboost Classifier. **cancerstage_I**: cancer stage I, **cancerstage_IV**: cancer stage IV, **servicecat_2**: public care service, **topogroup_C61**: cancer topography ICD C-61 (malignant neoplasm of prostate), **rrasofserv_RRAS06**: regional net of healthcare (service) 06, **servicecat_1**: private care service, **habilit_H7**: qualification H7 CACON with Pediatric Oncology Service, **topogroup_C73**: cancer topography ICD C-73 (malignant neoplasm of thyroid gland), **cancerstage_II**: cancer stage II, **habilit_H6**: qualification H6 CACON, **habilit_H9**: qualification H9 9 - UNACON with Radiotherapy and Hematology Services, **medsvtodiag**: difference in days between first medical appointment dates and diagnosis, **topogroup_C50**: cancer topography ICD C-50 (malignant neoplasm of breast), **age_70+**: age group of 70 years or more), **rrasofserv_RRAS09**: regional net of healthcare (service) 09, **morpho_M80703**: cancer morphology 80,703 (squamous cell carcinoma, NOS), **rras_R13**: regional net of healthcare (residence) 13, **rrasofserv_RRAS14**: regional net of healthcare (service) 14, **rrasofserv_RRAS02**: regional net of healthcare (service) 02.

Table 5
Comparison of the predictive performance between the specific algorithms for each type of cancer and the general algorithm.

Cancer Type	Model	Test size	Real Positive	True Positive	False Positive	True Negative	False Negative	Precision	Recall	AUC-ROC
Bronchus and	General	486	367	340	35	84	27	0.9067	0.9264	0.9265
Lung	Specific	542	401	367	44	97	34	0.8929	0.9152	0.8993
Breast	General	1192	206	146	29	957	60	0.8343	0.7087	0.9460
	Specific	1538	384	277	51	1103	107	0.8445	0.7214	0.9471
Stomach	General	383	277	258	26	80	19	0.9085	0.9314	0.9255
	Specific	409	289	270	59	61	19	0.8207	0.9343	0.8658
Colon	General	468	241	200	36	191	41	0.8475	0.8299	0.9241
	Colon	450	228	177	58	164	51	0.7532	0.7763	0.8717
Rectum	General	319	197	177	26	96	20	0.8719	0.8985	0.9163
	Colon	359	214	196	39	106	18	0.8340	0.9159	0.9230
Prostate	General	1192	206	146	29	957	60	0.8343	0.7087	0.9460
	Specific	1139	199	149	40	900	50	0.7884	0.7487	0.9552
Cervix Uteri	General	326	215	177	21	90	38	0.8939	0.8233	0.8850
	Specific	307	183	170	42	82	13	0.8164	0.9235	0.9173

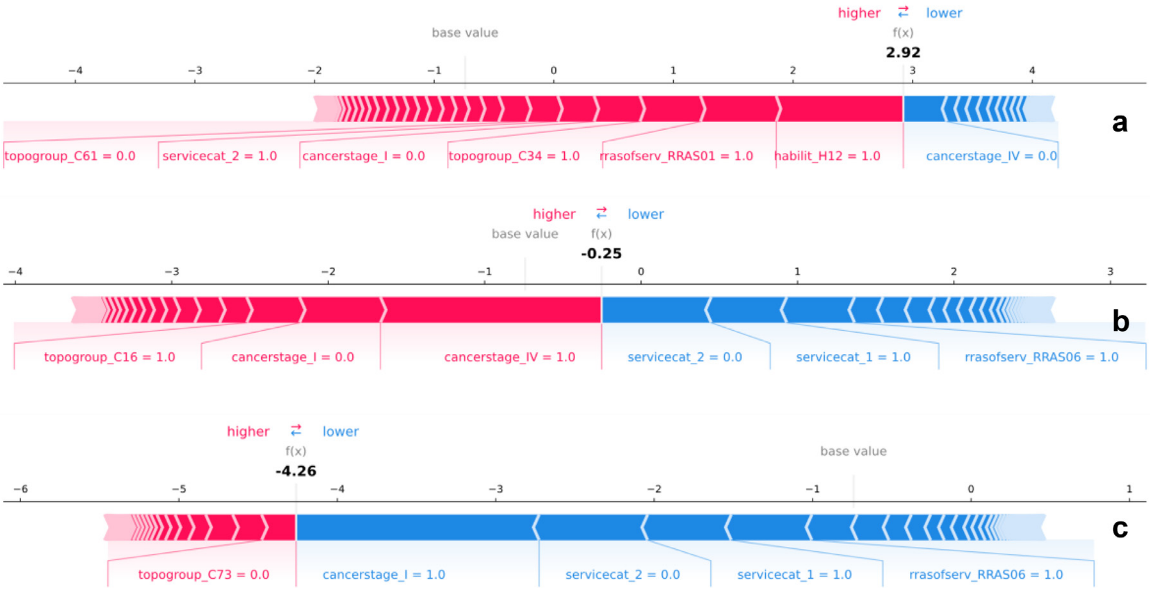

Fig. 4. Main predictors of risk of death from cancer between 12 and 24 months after diagnosis for three randomly selected individuals: a) high risk of death (true positive with 0.972 score), b) medium risk of death (false negative with 0.478 score) and c) low risk of death (true negative with 0.017 score), general model with Catboost Classifier. **Patient a) topogroup_C61:** cancer topography ICD C-61 (malignant neoplasm of prostate), **servicecat_2:** public care service, **cancer_stage1:** cancer stage I, **topogroup_C34:** cancer topography ICD C-34 (malignant neoplasm of bronchus and lung), **rrasofserv_RRAS01:** regional net of healthcare (service) 01, **habilit_H12:** qualification H12 UNACON with Hematology and Pediatric Oncology Services, **cancerstage_IV:** cancer stage I. **Patient b) servicecat_1:** private care service, **morpho_80,703:** cancer morphology 80,703 (squamous cell carcinoma, NOS), **cancerstage_I:** cancer stage I, **cancerstage_IV:** cancer stage IV, **servicecat_2:** public private care service, **rrasofserv_RRAS06:** regional net of healthcare (service) 06. **Patient c) topogroup_C73:** cancer topography ICD C-73 (malignant neoplasm of thyroid gland), **cancerstage_I:** cancer stage I, **servicecat_2:** public care service, **servicecat_1:** private care service, **rrasofserv_RRAS06:** regional net of healthcare (service) 06. Zero value are interpreted as the absence of the characteristic and one as the presence.

4. Conclusion

In conclusion, the nine final models developed for predicting risk of death in cancer patients presented high predictive performance. The algorithms can be an important tool to help prioritize treatment decisions and patient allocation in cancer treatments, especially in low-income regions. Future work should explore the proposed methodological structure and evaluate its predictive performance in new settings with different routinely collected data.

Ethical statement

This work was evaluated and approved by the Research Ethics Committee of the Faculty of Public Health of the University of São Paulo (CAAE: 65,375,722.9.0000.5421)

Data and code availability

The main results of this research were published in this article and in supplementary appendix A and B. The RHC/FOSP data are publicly available in https://www.fosp.saude.sp.gov.br/fosp/diretoria-adjunta-de-informacao-e-epidemiologia/rhc-registro-hospitalar-de-cancer/. The code developed for predictive modeling can be obtained upon request.

Funding

This work was supported by the São Paulo State Health Department, Special Health Fund for Mass Immunization and Disease Control (FESIMA/SES/SP).

Declaration of Competing Interest

The authors declare that they have no known competing financial interests or personal relationships that could have appeared to influence the work reported in this paper.

Data availability

The RHC/FOSP is publicly available on FOSP website. The code developed for predictive modeling can be obtained upon request.

Acknowledgement

We would like to acknowledge the São Paulo State Health Department, Special Health Fund for Mass Immunization and Disease Control (FESIMA/SES/SP) for supporting and funding this research.

Supplementary materials

Supplementary material associated with this article can be found, in the online version, at doi:10.1016/j.ailsci.2023.100061.

References

[1] Patel A. Benign vs Malignant Tumors. JAMA Oncol 2020;6(9) 1488–1488.
[2] Thuler LCS, Sant'Ana DR, Rezende MCR. Abc do câncer: abordagens básicas para o controle do câncer. ABC do câncer: abordagens para o controle do câncer; 2011. pages 127–127.
[3] World Health Organization (2022). Fact sheets: cancer.
[4] INCA (2019). Estimativa 2020: incidência de câncer no Brasil.
[5] Ministério da Saúde, Brasil. (2022). Sistema de informação sobre mortalidade (SIM).
[6] Bray F, Ferlay J, Soerjomataram I, Siegel RL, Torre LA, Jemal A. Global cancer statistics 2018: Globocan estimates of incidence and mortality worldwide for 36 cancers in 185 countries. CA 2018;68(6):394–424 [1].
[7] Iqbal MJ, Javed Z, Sadia H, Qureshi IA, Irshad A, Ahmed R, Malik K, Raza S, Abbas A, Pezzani R, et al. Clinical applications of artificial intelligence and machine learning in cancer diagnosis: looking into the future. Cancer Cell Int 2021;21(1):1–11.
[8] Secretaria de Estado da Saúde. (2022). Fundação Oncocentro de São Paulo. Registro hospitalar de câncer: banco de dados. São Paulo, Brasil.
[9] Lavras C. Atenção primária à saúde e a organização de redes regionais de atenção à saúde no brasil, 20. Saúde e Sociedade; 2011. p. 867–74.
[10] Prokhorenkova L, Gusev G, Vorobev A, Dorogush AV, Gulin A. CatBoost: unbiased boosting with categorical features. In: Advances in neural information processing systems; 2018. p. 31.

[11] Chen T, Guestrin C. XGBoost: A Scalable Tree Boosting System. In: Proceedings of the 22nd ACM SIGKDD International Conference on Knowledge Discovery and Data Mining. New York, NY, USA: ACM; 2016. p. 785–94. doi:10.1145/2939672.2939785.

[12] Ke G, Meng Q, Finley T, Wang T, Chen W, Ma W, Liu T-Y. Lightgbm: A highly efficient gradient boosting decision tree. Adv Neur Inform Process Syst 2017;30:3146–54.

[13] Pedregosa F, Varoquaux G, Gramfort A, Michel V, Thirion B, Grisel O, Duchesnay E. Scikit-learn: Machine learning in Python. J Mach Learn Res 2011;12:2825–30.

[14] Bergstra J, Yamins D, Cox DD. Making a Science of Model Search: Hyperparameter Optimization in Hundreds of Dimensions for Vision Architectures. In: To appear in Proc. of the 30th International Conference on Machine Learning (ICML 2013); 2013.

[15] Kursa MB, Rudnicki WR. Feature Selection with the Boruta Package. J Stat Softw 2010;36(11):1–13. doi:10.18637/jss.v036.i11.

[16] Lundberg S, Lee S-I. A unified approach to interpreting model predictions. NIPS; 2017.

[17] Lundberg SM, Nair B, Vavilala MS, et al. Explainable machine-learning predictions for the prevention of hypoxaemia during surgery. Nat Biomed Eng 2018;2:749–60. doi:10.1038/s41551-018-0304-0.

[18] Lundberg SM, Erion G, Chen H, et al. From local explanations to global understanding with explainable AI for trees. Nat Mach Intell 2020;2:56–67. doi:10.1038/s42256-019-0138-9.

[19] Moons KGM, et al. Transparent reporting of a multivariable prediction model for individual prognosis or diagnosis (TRIPOD): Explanation and elaboration. Ann Intern Med 2015;162(1):W1–73.

[20] Sharma A, Rani R. A Systematic Review of Applications of Machine Learning in Cancer Prediction and Diagnosis. Arch Computat Methods Eng 2021;28:4875–96. doi:10.1007/s11831-021-09556-z.

[21] Kumar Y, Gupta S, Singla R, et al. A Systematic Review of Artificial Intelligence Techniques in Cancer Prediction and Diagnosis. Arch Computat Methods Eng 2022;29:2043–70. doi:10.1007/s11831-021-09648-w.